

Elsevier Editorial System(tm) for Global and Planetary Change

Manuscript Draft

Manuscript Number: GLOPLACHA-D-07-00025R1

Title: HISTORICAL BEHAVIOUR OF DOME C AND TALOS DOME (EAST ANTARCTICA) AS INVESTIGATED BY SNOW ACCUMULATION AND ICE VELOCITY MEASUREMENTS

Article Type: Research Paper

Keywords: geophysical survey; ice divide; snow accumulation; Talos Dome; Dome C; East Antarctica

Corresponding Author: Massimo Frezzotti,

Corresponding Author's Institution: ENEA

First Author: Stefano Urbini

Order of Authors: Stefano Urbini; Massimo Frezzotti; Stefano Gandolfi; Christian Vincent; Claudio Scarchilli; Luca Vittuari; Michel Fily

Abstract: Ice divide-dome behaviour is used for ice sheet mass balance studies and interpretation of ice core records. In order to characterize the historical behaviour (last 400 yrs) of Dome C and Talos Dome (East Antarctica), ice velocities have been measured since 1996 using a GPS system, and the palaeo spatial variability of snow accumulation has been surveyed using snow radar and firn cores. The snow accumulation distribution of both domes indicates distributions of accumulation that are non-symmetrical in relation to dome morphology. Changes in spatial distributions have been observed over the last few centuries, with a decrease in snow accumulation gradient along the wind direction at Talos Dome and a counter-clockwise rotation of accumulation distribution in the northern part of Dome C. Observations at Dome C reveal a significant increase in accumulation since the 1950s, which could correlate to altered snow accumulation patterns due to changes in snowfall trajectory. Snow accumulation mechanisms are different at the two domes: a wind-driven snow accumulation process operates at Talos Dome, whereas snowfall trajectory direction is the main factor at Dome C. Repeated GPS measurements made at Talos Dome have highlighted changes in ice velocity, with a deceleration in the NE portion, acceleration in the SW portion and

migration of dome summit, which are apparently correlated with changes in accumulation distribution. The observed behaviour in accumulation and velocity indicate that even the most remote areas of East Antarctica have changed from a decadal to secular scale.

Dear Prof. Paolo Pirazzoli
Editor
Global and Planetary Change

Enclosed is the revised manuscript GLOPLACHA-D-07-00025, the Reviews comments have been taken into account in this revised manuscript, in particular:

Title has been changed and abstract and conclusion have been improved.

Editing error on manuscript has been corrected and figures 4 and 7 have been improved.

Relationship between depth and age has been improved.

Conclusion has been shortening.

We think that this new manuscript address all the remarks made by the reviewers and we hope that it will be accepted for publication in the Global and Planetary Change

Very sincerely

Massimo Frezzotti

Detailed response to Reviewer

Reviewer #2: But after reading the paper I was convinced that the conclusions are fair. But the title indicate that the results are good, but your conclusions are speculative. Thus I recommend that you stand up for your conclusion and change the title and the abstract.

On our opinion conclusions are well supported by results, however we have shortening and changed title and improved abstract and conclusion.

Reviewer #2: The radar data is the key information to the paper and it is well handled and the results are very good. 800 km of data is a lot though the distances are large in the area. The firm coring is based on standard techniques and are used to calibrate the GPR-data. They are rather few, but if the signal is strong from the identified layers it may be sufficient with a limited number of cores. The paper does not really say that but it make sense. The velocity measurements are more problematic as they are few and show strange things like major shifts in direction of movement and the uncertainties in these long distance measurements are significant. Though the results support the conclusions I question whether this section is necessary to the paper. Omitting this part would probably make the paper even more convincing.

It is a first time in Antarctica that dome velocities have been measured for 5 time at distance of 10 years, and are therefore unique (as pointed out by Reviewer #4). On our opinion and on the base of other reviewer comments we do not think it is a good idea to omit this part. Change in accumulation and velocity are complementary to demonstrate the migration of the ice domes through the last 400 years.

Reviewer #3:

Minor comments

P 7: 3.1.1 frezzotti 2004 is not in press (it is published),
Frezzotti et al. in press is 2007 JGR (text has been changed) and not Frezzotti et al. 2004a
Ann. Glaciol or Frezzotti et al. 2004b Climate Dynamics

Figure 4 is not net (the digits and axis are not easy to read)
We have improved the figure and we suggest printing the figure at full page width.

Reviewer #4: Overall

In this paper the authors use snow accumulation and ice velocity data from two East Antarctic ice domes to demonstrate the migration of the ice domes through the last 400 years. The data sets used for this; stake farms, ice cores and snow radar are collected by one of the most extensive national glaciology field programs in Antarctica and are therefore unique. This group has done an impressive job using and interpreting these extensive data sets in an interesting way.

The paper is generally well -written. However, the paper suffers somewhat from the fact that there are so much data on hand that it is difficult for the reader to always follow which data

have been used for what analyses and the reasoning behind. Therefore it is also hard to easily judge how reliable the conclusions are. Below I have suggested some particular areas that have to be improved and once that is accomplished I recommend that this paper is accepted for publication.

The text has been improved following the indication of reviewer and conclusion has been shortening.

Specific comments

There are some confusion in the text between what are "Methods" and what are "Results".

Comparison from core and GPR has been moved to result as suggested.

As I have already pointed out above I do not feel that it is easy to follow what data have been used for what. Unfortunately, the figures are not particularly helpful with this matter. One of the most crucial points that the results in this paper depends on is how the depth-age transfer function from the GPR data was derived. It is not easy to follow which of the different dating horizons are used for what just by reading the text. Would it be possible to compile all that information in a table? For instance I miss information about what "important past volcanic events" was used for dating. I think that it is necessary to guide the reader through some of this in a better way. In that table information about dating errors could also be added. I think the amount of text will decrease and it will be easier to read.

The text has been rewritten and some shortening following the suggestion. In particular detail of depth-age function, dating errors and past volcanic events has been improved.

Minor comments

AD is used inconsistently both before and after the year.

Text has been modified

p. 6 , line 9. Rennick Basin should appear on the map (fig. 3).

Rennick Basin is out of Figure 3, text has been modified

p. 10 line 30: should be "1580 AD-1710 AD and 1710 AD-present."

Text has been modified

p. 11, line 6: please use abbreviations for N, and E since you have used it for NE already.

Text has been modified

Fig. 2. This figure needs some better explanation in the caption. The text does not seem to match what is displayed in the figure.

Figure 2 caption has been improved.

1 **HISTORICAL BEHAVIOUR OF DOME C AND TALOS DOME (EAST ANTARCTICA)**
2 **AS INVESTIGATED BY SNOW ACCUMULATION AND ICE VELOCITY**
3 **MEASUREMENTS**

4
5 Stefano Urbini¹, Massimo Frezzotti², Stefano Gandolfi³, Christian Vincent⁴, Claudio
6 Scarchilli², Luca Vittuari³, Michel Fily⁴

7
8 ¹ Istituto Nazionale di Geofisica e Vulcanologia, Via di Vigna Murata 605, 00143 Roma,
9 Italy

10 ² Ente per le Nuove Tecnologie, l'Energia e l'Ambiente, Via Anguillarese, 301, 00123
11 Roma, Italy

12 ³ Dipartimento di Ingegneria delle Strutture, dei Trasporti, delle Acque, del Rilevamento,
13 del Territorio, V.le Risorgimento 2, 40086 Bologna, Italy

14 ⁴ Laboratoire de Glaciologie et Géophysique de l'Environnement, CNRS-UJF, 54 rue
15 Molière, Grenoble, France

16
17 Corresponding author:

18 Massimo Frezzotti

19 Tel: +39 06 30483271

20 Fax: +39 06 30486678

21 e-mail: frezzotti@casaccia.enea.it

1 **Abstract.** Ice divide-dome behaviour is used for ice sheet mass balance studies
2 and interpretation of ice core records. In order to characterize the historical behaviour
3 (last 400 yrs) of Dome C and Talos Dome (East Antarctica), ice velocities have been
4 measured since 1996 using a GPS system, and the palaeo spatial variability of snow
5 accumulation has been surveyed using snow radar and firn cores. The snow
6 accumulation distribution of both domes indicates distributions of accumulation that are
7 non-symmetrical in relation to dome morphology. Changes in spatial distributions have
8 been observed over the last few centuries, with a decrease in snow accumulation
9 gradient along the wind direction at Talos Dome and a counter-clockwise rotation of
10 accumulation distribution in the northern part of Dome C. Observations at Dome C reveal
11 a significant increase in accumulation since the 1950s, which could correlate to altered
12 snow accumulation patterns due to changes in snowfall trajectory. Snow accumulation
13 mechanisms are different at the two domes: a wind-driven snow accumulation process
14 operates at Talos Dome, whereas snowfall trajectory direction is the main factor at Dome
15 C. Repeated GPS measurements made at Talos Dome have highlighted changes in ice
16 velocity, with a deceleration in the NE portion, acceleration in the SW portion and
17 migration of dome summit, which are apparently correlated with changes in accumulation
18 distribution. The observed behaviour in accumulation and velocity indicate that even the
19 most remote areas of East Antarctica have changed from a decadal to secular scale.

20
21 *Keywords:* geophysical survey; ice divide; snow accumulation; Talos Dome; Dome C;
22 East Antarctica

23 **1. Introduction**

24
25 One of the most extreme environments on the Earth's surface is the ice divide
26 extending from Dronning Maud Land (DML) to Talos Dome (TD) in inner East Antarctica
27 (Fig. 1). Due to extremely difficult field conditions in the inner part of East Antarctica, the
28 accumulation pattern and evolution of the dome-ice divide is poorly known. The Earth's
29 oldest ice cores were obtained along or near this ice divide (EPICA DML, Dome Fuji,
30 EPICA Dome C, Vostok). Dome C (DC), Antarctica's fourth highest dome (3233 m), is
31 about 1200 km from the Southern Ocean. The French-Italian Concordia Station
32 (123°20'52"E, 75°06'04"S), where the EPICA (European Project for Ice Coring in

1 Antarctica) drilling site is located, is about 1.4 km west of the DC surface summit. TD is
2 an ice dome on the edge of the East Antarctic plateau (159°04'21"E, 72°47'17"S; 2318
3 m), about 1100 km East of DC (Fig. 1) and about 280 km from the Southern Ocean and
4 Ross Sea.

5 In December 2004 a 3270 m deep ice core was recovered at DC within the
6 framework of EPICA. This core provides the oldest existing ice climate record, extending
7 to 740,000 years before the present (EPICA community, 2004). In 2004, a new ice coring
8 project, TALDICE (Talos Dome Ice Core Project), was started at TD with the aim of
9 recovering 1550 m of ice that spans the last 120,000 years (Frezzotti et al., 2004a). Ice
10 divide-dome migration cannot be directly detected. However, the stability of the dome and
11 position of the ice divide must be known in order to accurately interpret ice core records
12 and to complete ice sheet mass balance studies. Models of depth-age relations for deep
13 ice cores are sensitive to migration of the dome position (Anandakrishnan et al., 1998).
14 Ice divide migration is also important in determining the input parameter of large Antarctic
15 drainage basins. The behaviour of an ice divide is driven by its accumulation rate history
16 and spatial pattern and conditions at ice sheet boundaries (e.g. Frezzotti et al., 2004a;
17 Hindmarsh, 1996; Nereson et al., 1998). Indeed, surface elevations at DC, Vostok and
18 Dome Fuji have varied by up to 100-150 m between glacial and interglacial periods due
19 to changes in accumulation (Ritz et al., 2001).

20 The low slope (less than one decimetre per km) of the East Antarctic domes and
21 their surface morphology at meter scale (e.g., sastrugi) makes it very difficult to determine
22 the summit point of the dome and its migration over time.

23 The objective of this paper is to provide information on the historical behaviour of
24 DC and TD using snow accumulation distribution during the last 400 years as revealed by
25 detailed snow accumulation, radar derived isochrones and ice dynamic changes based
26 on ice velocity measurements made over the last 10 years.

27 These data should be very useful in the future for determining changes in mass
28 balance and thickness in these areas and detecting the possible impact of climate
29 change to the ice core. DC and TD are also interesting sites for comparisons with satellite
30 observations and numerical modelling.

31

1

2 **2. Materials and Methods**

3

4 Internal layers of strong radar that are reflectivity observed with Ground
5 Penetrating Radar (GPR) are isochronous, and surveys along continuous profiles provide
6 detailed information on spatial variability in snow accumulation (e.g., Richardson et al.,
7 1997; Vaughan et al., 1999; Eisen et al., 2004; Spikes et al., 2004; Frezzotti et al., 2002;
8 2005). For the purposes of this study, sixteen shallow snow-firn cores were drilled in the
9 DC area and six in the TD area (Frezzotti et al., 2004a; 2005; 2007; Vincent and
10 Pourchet, 2000). All core sites were linked through GPR and GPS (Global Positioning
11 System) surveys in order to gain detailed insight into the spatial variability of snow
12 accumulation. Strain networks established in the DC and TD areas have been surveyed
13 (using static GPS and DORIS measurements) since 1993 (Frezzotti et al., 2004a; Vittuari
14 et al., 2004).

15

16 2.1 Snow accumulation and isochrones

17

18 A total of 800 km of GPR and kinematic GPS surveys (500 km at DC, 300 km at TD) were
19 carried out within a 25 km radius of the domes. GPS surveys were integrated with
20 previous surveys to create a detailed topographic map (Frezzotti et al., 2004a; Cefalo et
21 al., 1996; Capra et al., 2000). The accuracy of the GPS elevation profile is about 10 cm;
22 the interpolation process reduces accuracy to about 20 cm in the maps. Due to a very low
23 slope in the summit area, surface morphology at meter scale (e.g., sastrugi, barchans
24 etc.) and instrumental error, it is very difficult to define the precise position of the dome
25 summit. Therefore, we identified the dome summit as the area inside the highest contour
26 line.

27 GPR data acquisition was performed using a GSSI Sir10B unit equipped with two
28 monostatic antennas with a central frequency of 400 and 900 MHz at DC and one
29 monostatic antenna with a central frequency of 200 MHz at TD. The traces were recorded
30 at about one scan per metre in a 150 ns time window for the 900 MHz antenna (14-15 m),
31 a 350 ns time window for the 400 MHz antenna (33-35 m investigation depth) and a 750

1 ns time window for the 200 MHz antenna (60-70 m). A rate of 4 scans s^{-1} and 512
2 samples per trace was chosen for antennas. Post-processing of GPR data involved gain
3 ranging, low and high bandpass filtering and trace stacking. The recorded two-way travel
4 times (TWT) were converted to depths following the density-depth information-based
5 methodology outlined in Frezzotti et al. (2002). Density information was obtained from 16
6 firn cores (from 6 to 50 m deep) and 1 trench (3 m deep) at DC and 3 firn/ice cores (from
7 26 to 89 m deep) and 2 trenches (2.5 m deep) at TD. Density profile analysis revealed no
8 detectable geographical variation in density or compaction within the dome areas. All
9 density data were therefore fitted with a second-order polynomial function for each dome
10 area; this yielded a correlation coefficient (R^2) of more than 0.9 for both measured and
11 computed densities. The integration of density measurements yielded cumulative mass
12 as a density-depth function along each radar profile. Given the small differences in
13 density at isochrone depths (max difference 1 m), the snow compaction rate difference
14 between sites is negligible for calculation purposes. Layer thinning due to vertical strain
15 can be also considered to be negligible ($3 \cdot 10^{-5} \text{ yr}^{-1}$).

16 Six continuous internal layers were tracked along all profiles at DC (L1 and L2 with the
17 900 MHz antenna and L3, L4, L5 and L6 with the 400 MHz antenna) and four along
18 profiles at TD (L3, L4, L5 and L6 with the 200 MHz antenna). Depth uncertainty in GPR
19 data was estimated to be about ± 14 cm for data acquired with the 200 MHz antenna (TD),
20 ± 6 cm for data acquired with the 400 MHz antenna and ± 3 cm for the 900 MHz antenna
21 (DC). Layer depths measured at intersecting points were in good agreement (± 25 cm for
22 200 MHz, ± 15 cm for 400 MHz and ± 10 cm for 900 MHz). Layer data were mapped using
23 Kriging interpolation (linear semivariogram, nugget equal to 0.003) to draw snow
24 accumulation and palaeo maps.

25 Stratigraphic dating of EPICA (Udisti et al., 2000; Castellano et al., 2005), through non-
26 sea-salt (nss) SO_4^{2-} spikes from the past volcanic events (Pinatubo 1992 AD, Agung 1964
27 AD, Krakatua 1887 AD, Tambora 1816 AD, Jorull-Taal 1758 AD, Serua 1696 AD,
28 Huaynaputina 1601 AD, Kwuue 1460 AD), was used to establish the depth-age function
29 of the GPR isochrones at DC. Analogously at TD, the age of GPR isochrones was
30 estimated using stratigraphic dating of TD core (Stenni et al., 2002) through seasonal
31 variations in nss SO_4^{2-} concentrations coupled with the identification of tritium marker

1 levels (1965-66 AD) and nssSO_4^{2-} spikes from past volcanic events (Pinatubo 1992 AD,
2 Agung 1964 AD, Rabaul 1938 AD, Krakatua 1887 AD, Consequina 1837 AD, Tambora
3 1816 AD, Serua 1696 AD, Huaynaputina 1601 AD, Kwuae 1460 AD).
4 According to the defined depth-age function, the depth of layers L1 (5.7 m) and L2 (9.1
5 m) at the EPICA site was dated to 1921 ± 3 and 1869 ± 3 AD, respectively; layer L5 (16.4
6 m) was dated to 1739 ± 7 AD, whereas the deepest layer L6 (23.2 m) was dated to 1602 ± 9
7 AD. Previously, Frezzotti et al. (2004a) used the same methodology to establish a depth-
8 age function at TD core sites; S1 (14.8 m) dates to 1920 ± 2 AD, S2 (26.7 m) to 1835 ± 2
9 AD, S3 (49.3 m) to 1635 ± 5 AD and the deepest traceable S4 (61.2 m) to 1525 ± 5 AD.
10 The snow accumulation rate of 16 firn cores within a 25 km radius of DC (Frezzotti et al.,
11 2005; Vincent and Pourchet, 2000) was determined for the last 50 years using β and
12 tritium peaks from 1965-66 AD atmospheric thermonuclear bomb tests and for the past
13 two centuries using the Tambora marker (1816 AD). The experimental error ($\pm \sigma_e$) in
14 calculated snow accumulation rates using firn core is estimated to be less than 10% for
15 β -radioactivity (1965-2000 AD) and less than 5% for both the tritium period (1966-1998
16 AD) and the period since Tambora (1816-1998 AD; Fig. 2).

17

18 2.2 Velocity measurements

19 Surface strain networks consisted of 9 stakes at TD and 37 stakes at DC. Stakes were
20 placed 8 km away from the centre of TD and 3, 6, 12.5 and 25 km from the centre of DC.
21 GPS measurements of the networks were completed 4 times at TD (Table 1) and 2 times
22 at DC. Reference poles (located close to the dome summits) were positioned on the basis
23 of static GPS measurements; the Terra Nova Bay permanent GPS station was the base
24 station for TD, while DORIS was the base station for DC. Process details are reported
25 elsewhere (Frezzotti et al., 2004a; Vittuari et al., 2004). Here, we present the results of 4
26 repeated measurements performed at TD (Table 1) between the end of 1996 and the
27 beginning of 2005 (Nov 1996; Dec 1998; Jan 2002; Jan 2005). The estimated uncertainty
28 between two GPS positions at TD is ~ 28 mm, with an uncertainty of less than 10 mm yr^{-1}
29 for 1998-2002 measurements and $\sim 14 \text{ mm yr}^{-1}$ for 1996-98 and 2002-2005
30 measurements; the uncertainty in acceleration is estimated to be $\sim 2.5 \text{ mm yr}^{-2}$ for
31 measurements taken 5.6 years apart.

1

2 **3. Results and discussion**

3

4 3.1 Spatial and temporal accumulation distribution

5

6 *3.1.1 Talos Dome*

7

8 Based on the depth distribution of snow layers, Frezzotti et al. (2004a; 2007) found that
9 accumulation decreases downwind of TD (N-NE) and is higher in the SSW sector (Fig. 3).
10 TD surface contour lines are elliptical and elongated in a NW-SE direction; the NW and
11 NE slopes are steeper. The elongation direction of the dome is perpendicular to the
12 prevalent wind direction and parallel to both the outcropping Outback Nunataks (50 km
13 North to TD) and the sharp NW-SE ridge in the bedrock. At TD, wind blows uphill from the
14 SW with a gradient of $1\text{--}2\text{ m km}^{-1}$ for a distance of 100 km. As pointed out by Frezzotti et
15 al. (2007), the higher accumulation in the SSW sector is correlated with reduced wind-
16 driven sublimation in this area, which is due to the positive slope gradient that reduces
17 wind velocities. The lower accumulation in the downwind sector is ascribable to an
18 increase in wind-driven sublimation, which was determined by the increase in the surface
19 slope toward the Southern Ocean (Figs. 1 and 3).

20 Analysis of the palaeo-accumulation map (Figs. 4 and 5) shows the spatial and temporal
21 variability of accumulation over the last four centuries. During the period 1835-1920 AD,
22 the accumulation value is significantly lower compared to the previous (1635-1835 AD)
23 and subsequent (1920-2001 AD) dates in the SW portion, whereas accumulation in the
24 NE sector is more constant across periods. The decrease in the SW part significantly
25 reduces the accumulation gradient along the wind direction (Fig. 4) during the 1835-1920
26 AD period. An analysis of summit isochrone positions in the past reveals a possible SE
27 migration of about 3.5 m yr^{-1} since the deposition of layer S4 (1526 AD). The δD recorded
28 for the TD core shows a cooler condition and a decrease in snow accumulation during the
29 Little Ice Age (LIA), followed by an increasing trend in δD up to the 1920s-1930s and then
30 negative values during the periods 1930s-1996 AD. Cooler atmospheric temperature
31 conditions in the TD area during the LIA may have increased the persistence of katabatic

1 winds (Stenni et al., 2002). Precipitation reflects large (synoptic) scale phenomena
2 related to circulation on a global scale and is homogenous on a large scale (hundreds of
3 km²), but wind-driven sublimation phenomena determined by the surface slope along
4 prevailing wind directions have a considerable impact on the spatial distribution of snow
5 on short (tens of meters) and medium (kilometre) spatial scales (Frezzotti et al, 2004b;
6 2005; 2007). Changes in wind conditions could determine a decrease/increase in snow
7 accumulation in upwind/downwind areas. Accumulation records from stakes and firn
8 cores at the TD summit show increases over the past 200 years; the increase has been
9 more pronounced since the 1960s atomic bomb markers as compared to the previous
10 period from Tambora onward (1816-1965 AD). However, since the 1990s a decrease in
11 accumulation (about 10%) has been observed as compared to the 20th century average,
12 as computed from stake measurements (Frezzotti et al., 2007). Snow accumulation
13 measurements (4 stake farms and 5 firn cores) taken along the 500 km transect crossing
14 TD show no significant increases in accumulation over the last two centuries (Frezzotti et
15 al., 2007). In a previous paper, Stenni et al. (2002), who based their findings on a single
16 firn core, reported a decrease in accumulation during a part of the LIA (1643-1902 AD),
17 followed by an increment in accumulation of about 11% during the 20th century (1902-
18 1996 AD).

19

20 3.1.2 Dome C

21

22 Elevation contour lines (Fig. 6) show that the most prominent characteristic of the DC
23 surface is its elliptical shape, with the minor axis (NW-SE) being about 70% shorter than
24 the major (SW-NE) axis (Remy and Tabacco, 2000). The elongation direction of the
25 dome is parallel to the prevalent SW-NE wind direction (Frezzotti et al., 2005).
26 Comparison of snow accumulation of two cores (site A17 at DC), drilled tens of metres
27 apart, reveals an 11% difference in accumulation for the tritium/ β marker horizons.
28 Comparison of snow accumulation data derived from 16 firn core records (using atomic
29 bomb and Tambora markers) and from GPR isochrones (using EPICA depth-age
30 function) at DC shows good agreement within the experimental error (Fig. 2). The
31 difference of snow accumulation values between cores and snow radar data reflect

1 temporal and spatial differences among sample areas, snow accumulation variability at
2 the core scale and the increase in snow accumulation at DC since 1960 (Frezzotti et al.,
3 2005). The depth of GPR layers increases from South to North (up to 1.5 m in 50 km; Fig.
4 7). The deepening of layers and the related increase in accumulation is more pronounced
5 at the Concordia Station to the North. The depth increase is equivalent to a South-North
6 increase in snow accumulation rate of about $0.02 \pm 0.01 \text{ kg m}^{-2} \text{ yr}^{-1}$ per km from the South
7 to Concordia Station and about $0.08 \pm 0.01 \text{ kg m}^{-2} \text{ yr}^{-1}$ per km from the Concordia Station
8 to the North. The snow accumulation map and profile (Figs. 6 and 7) clearly show this
9 pattern, with a marked increase in accumulation in the northern part of DC. This
10 accumulation pattern was poorly defined by core data and snow radar L1 (dated to
11 $1921 \pm 3 \text{ AD}$) due to a “relatively larger error” (from ± 1.5 to $\pm 3.4 \text{ kg m}^{-2} \text{ yr}^{-1}$), with respect to
12 the local spatial variability in snow accumulation (about $\pm 0.9 \text{ kg m}^{-2} \text{ yr}^{-1}$, 3%) relative to
13 the accumulation gradient (about $3 \text{ kg m}^{-2} \text{ yr}^{-1}$ per 50 km) and the observation time span
14 (Fig. 2). This spatial snow accumulation gradient is present in all layers but is more
15 observable in the deepest layers.

16 The following observations, in addition to the local accumulation pattern discussed
17 above, indicate that DC is a key area that marks the change in accumulation distribution,
18 with a decrease in the accumulation gradient to the South and East:

- 19 • based on the Tambora marker (Frezzotti et al., 2005; Legrand and Delmas,
20 1987), the accumulation gradient is $0.01 \text{ kg m}^{-2} \text{ yr}^{-1} \text{ km}^{-1}$ between Vostok and DC
21 (650 km) and $0.08 \text{ kg m}^{-2} \text{ yr}^{-1} \text{ km}^{-1}$ between DC and old Dome C (55 km NE of
22 DC, Fig. 1);
- 23 • SW-NE deep ice-penetrating radar transect (800 km long) centred at DC
24 (Siegert, 2003) shows a relatively abrupt increase in the accumulation rate just
25 NE of DC;
- 26 • present regional accumulation data from West (Young et al., 1982) to East
27 (Frezzotti et al., 2004b) show a decrease in accumulation in the eastern part of
28 DC; and
- 29 • $\delta^{18}\text{O}$ values for the sites East of DC along the DC - Terra Nova Bay transect are
30 more negative than those for DC and the West and North sides, probably due to

1 isotope depletion in precipitation, which is induced by an orographic “shadowing”
2 effect in the eastern DC area (Magand et al., 2004).

3
4 Using nssSO_4 volcanic spikes (Castellano et al., 2005) from the last 500 years, an
5 analysis of snow accumulation in the EPICA ECD96 core shows that accumulation was
6 lower ($<25 \text{ kg m}^{-2} \text{ yr}^{-1}$) during the Kuwae-Tambora period (1460-1816 AD) than from
7 Tambora to the present ($>26 \text{ kgm}^{-2} \text{ yr}^{-1}$). Frezzotti et al. (2005) used a stake network
8 within 25 km of Concordia Station ($39 \text{ kg m}^{-2} \text{ yr}^{-1}$; 1996-1999 AD) and atomic bomb
9 markers for 18 firn cores ($28.3 \text{ kg m}^{-2} \text{ yr}^{-1}$ 1965-2000 AD) and observed a recent temporal
10 increase in snow accumulation compared to the Tambora period ($25.3 \text{ kg m}^{-2} \text{ yr}^{-1}$ 1816-
11 1998 AD). A stake farm network that was established in 2004 close to Concordia and re-
12 measured seasonally, within the framework of the Station observatory ([http://www-
13 lgge.obs.ujf-grenoble.fr/~christo/glacioclim/samba](http://www-lgge.obs.ujf-grenoble.fr/~christo/glacioclim/samba)), confirms the significant increase in
14 the observed accumulation ($\sim 32 \text{ kg m}^{-2} \text{ yr}^{-1}$). Moreover, temporal variability of deuterium
15 excess (proxy of oceanic moisture source conditions) at the old DC site and EPICA
16 ECD96 cores (Lorius et al., 1979; Stenni et al., 2001) and sodium at the EDC96 core
17 (proxy of marine aerosol; Röthlisberger et al., 2000) shows an atmospheric moisture
18 source variation between 1580-1710 AD and 1710 AD – to the present (Fig. 8).

19 Backward air parcel trajectories reveal that the resulting snowfall trajectories at DC come
20 from the North (Reijmer et al., 2002). The present-day and palaeo accumulation is driven
21 by the direction of snowfall and its interaction with “orography”. The suggested changes in
22 the eccentricity of the polar vortex during past glacial periods (Delmonte et al., 2004;
23 Udisti et al., 2004), coupled with a change in the atmospheric pathway of snowfall (from N
24 to NE and/or E), may have influenced the distribution of accumulation and shape/position
25 of the dome. A reconstruction of the ice sheet accumulation rate at Ridge B shows that
26 the western flank of the ice divide experiences markedly more accumulation than the
27 East; moreover, records for the last 124 kyrs show temporal and spatial variability around
28 the Ridge B ice divide (Leysinger Vieli et al., 2004).

29 An analysis of GPR-based palaeo-accumulation distribution data (Figs. 7, 8 and 9)
30 reveals a general pattern of increase and decrease in accumulation rates, with the lowest
31 value falling in the period 1602-1739 AD and the highest from 1739-1869 AD. Based on

1 palaeo-accumulation distribution data for the southern and eastern areas of DC, the
2 accumulation distribution does not appear to have changed significantly between the past
3 and present. In the northern part, by contrast, the palaeo-accumulation distribution
4 pattern shows a counter-clockwise rotation from East to West, with an increase in
5 asymmetry between the accumulation pattern and the morphology shape of the dome
6 (Fig. 9). Based on observations at different sites in East Antarctica (South Pole, DC, TC,
7 Vostok etc.), an increase in accumulation has occurred over the last two centuries and
8 during the period between the 1960s and 1990s, with cyclic variation at the decadal
9 scale. However, no significant increase has been observed since the 1990s at several
10 sites in East Antarctica (Frezzotti et al., 2005; 2007 and reference therein). Snowfall
11 accumulation across the continent has been investigated since the 1950s by combining
12 mode simulations and observations primarily from firn cores, and the research suggests
13 that there has been no substantial increase but rather a slight downturn in accumulation
14 in the past decade (Monaghan et al., 2006)

15 The significant increase in snow accumulation observed at DC since the 1990s, but not in
16 other East Antarctica sites, could be correlated with oddly increased precipitation at the
17 sites. However, a different snowfall trajectory could likewise have resulted in an increase
18 of accumulation, given the different spatial distribution at the dome site.

19
20

21 3.2 Ice velocity change

22

23 *3.2.1 Talos Dome*

24 At TD, the highest horizontal velocities were recorded for the “steeper” S-SW and
25 E-NE slopes, whereas the lowest horizontal velocities were recorded close to the dome
26 summit and along the SE ice divide (Frezzotti et al., 2004a). Data (Table 1, Fig. 5) reveals
27 deceleration from 5 ± 3 to 2 ± 3 mm yr⁻² in the sector from North to SE (from TD01 to TD05)
28 and acceleration from 1 ± 3 to 4 ± 3 mm yr⁻² in the sector from NW to South (from TD06 to
29 TD09). Although velocity changes below 3 mm yr⁻² fall within the margin of error due to
30 measurement uncertainty, the geographical distribution of all acceleration/deceleration
31 measurements are coherent at each site and are higher than the level of uncertainty in 5

1 out of 9 measurements (Table 1). The bearing rotates counter-clockwise in the North and
2 NW portions and clockwise in other sectors. The snow radar profile reveals an
3 approximately 10% increase in accumulation in the SW part. Due to the very low slope
4 gradient, it is difficult to evaluate changes in slope.

5 At the dome, where the surface slopes very little, the ice dynamics are very low
6 and appear to be a complex function of slope, ice thickness/bedrock conditions and the
7 snow accumulation rate distribution. It is difficult to determine the factors influencing the
8 absolute position of the dome because plate tectonics determines values that are similar
9 to or higher than the dome migration ascribable to glacio-climatological factors. In order to
10 determine absolute displacement through repeated surveys, the effects of the tectonic
11 motion of the Antarctic plate must be modelled and corrected. Our analysis takes into
12 account the tectonic displacement of the Antarctic plate extracted from the global model
13 Nuvel 1A - NNR 1991 (Altamini et al, 2002; Argus and Gordon, 1991) and verified within
14 Victoria Land through repeated GPS measurements of the Victoria Land deformation
15 network (VLNDEF). The main observable effect is induced by the rotational-translational
16 motion of the continent as a whole (Dietrich and Rulke, 2002; Negusini et al., 2005), with
17 the approximate motion of the continent that was extrapolated at TD01 being $\sim 15 \text{ mm yr}^{-1}$
18 with an azimuth of 141° . Acceleration-deceleration at TD occurs in a SW direction,
19 whereas the tectonic movement of the continent is at 90° in a SE direction.

21 3.2.2 Dome C

22 GPS measurements indicate that poles closest to the DC summit move up to a
23 few mm yr^{-1} , while poles located 25 km from the summit move up to 211 mm yr^{-1} (Vittuari
24 et al., 2004). Two years of continuous GPS measurements at the Concordia Station-
25 EPICA site allow the determination of absolute velocity to be $10.9 \pm 0.6 \text{ mm yr}^{-1}$ with a
26 direction of 302° . The absolute movement of DC is within the instrumental error of about
27 $\pm 7 \text{ mm yr}^{-1}$, and no absolute horizontal movement of the dome could be detected on the
28 basis of two measurements made 3 years apart (Vittuari et al., 2004). Within 25 km of
29 DC, the ice thickness and bedrock topography oscillate with amplitudes of up to $\pm 400 \text{ m}$,
30 with greater thicknesses observed to the North and lower thicknesses to the South
31 (Forieri et al., 2003). Balance velocity calculations based on the system proposed by

1 Legresy et al. (2000) are in agreement with ice velocity measurements and detection
2 limits. The greater thickness in the northern DC area compensates the relatively higher
3 accumulation in balance velocity. The combination of a low accumulation gradient (0.02-
4 $0.08 \text{ kg m}^{-2} \text{ yr}^{-1}$ per km) and slope (less than 0.5 m per km) and relatively large variations
5 in ice thickness (± 400 m) hinders the detection of ice velocity ($\pm 7 \text{ mm yr}^{-1}$) or strain rate
6 (about 10^{-5} yr^{-1}) differences using GPS or remote sensing surveys carried out 3 years
7 apart within 25 km of the summit. In the near future, repeat measurements of the DC
8 strain network will allow the detection of possible changes in ice velocity in the northern
9 sector of the dome, but only a fourth repetition taking place more than 15 years after the
10 first measurements will allow the detection of a possible velocity change.

11

12

13 **4. Conclusions**

14

15 The accumulation map obtained from snow radar data reveals a significant spatial
16 variability in the snow accumulation rate at Talos Dome and Dome C. Accumulation
17 distributions are not symmetrical in relation to dome morphology, and the accumulation
18 distribution pattern has changed over the last few centuries. At Talos Dome the
19 accumulation value for the period 1835-1920 AD is significantly lower than the values for
20 the previous (1635-1835 AD) and subsequent (1920-2001 AD) periods in the SW part,
21 whereas in the NE, accumulation in the same period is more similar to that observed for
22 the other two periods. The palaeo-accumulation distribution at Talos Dome shows a
23 decrease in the accumulation gradient along the wind direction, which could be due to
24 changes in the wind-driven accumulation process. Repeated GPS measurements made
25 at Talos Dome have highlighted changes in ice velocity, with a decrease in velocity in the
26 NE portion and an increase in the order of mm yr^{-2} in the SW portion. As a result of the
27 changed accumulation conditions, the Talos Dome summit has probably migrated to SE
28 in the last few centuries. Findings in the northern part of Dome C indicate that the
29 accumulation distribution has undergone a counter-clockwise rotation in the last 260
30 years (from 1739 AD to present) relative to the pattern of the previous 130 years (from
31 1602 to 1739 AD). At both domes, we observed a change in the distribution pattern at the

1 century scale and a significant increase in accumulation at Dome C since the 1990s,
2 which could be correlated with changes in snow accumulation patterns that reflect a
3 change in snowfall trajectory. The difference between present and past accumulation
4 reveals that the dynamics of the domes change from the decadal and century scales.
5 Snow accumulation distribution mechanisms are different at the two domes: a wind-driven
6 snow accumulation process operates at Talos Dome, whereas snowfall trajectory is the
7 main factor at Dome C.

8 The spatial variability at km scale of snow accumulation is very important on the
9 Antarctic Ice Sheet and also at the dome site and is of the same order of magnitude or
10 greater than temporal variability at the multi-decade/secular scale. Moreover, past
11 changes in snow accumulation distributions have consequences on the flow direction of
12 ice and dome-ice divide morphology and relationships (e.g., presence/absence of
13 saddles connecting the domes to the ice divides). The study of the position and
14 environmental characteristics of ice divides under the present climatic conditions will help
15 determine past variations in ice divides and dome positions.

16 The ongoing change of a dome-ice divide cannot be detected through annual-
17 scale measurements; rather, repeated measurements spanning several decades are
18 required.

19

20 **Acknowledgements**

21

22 Research was carried out in the framework of the Project on Glaciology of the PNRA-
23 MIUR and was financially supported by the PNRA Consortium through collaboration with
24 ENEA Roma. This paper is a French-Italian contribution to the ITASE and Concordia
25 Station projects and the EPICA and TALDICE projects. EPICA is a joint ESF (European
26 Science Foundation)/EU scientific programme funded by the European Commission and
27 by national contributions from Belgium, Denmark, France, Germany, Italy, the
28 Netherlands, Norway, Sweden, Switzerland and the United Kingdom. The present
29 research was made possible by the joint French-Italian Concordia Program, which
30 established and runs the permanent station Concordia at Dome C. Talos Dome Ice core
31 Project (TALDICE), a joint European programme, is funded by national contributions from

1 Italy, France, Germany, Switzerland and the United Kingdom. Main logistic support was
2 provided by PNRA. This is EPICA publication no. xx and TALDICE publication no yy.

5 **References**

- 6
- 7 Altamini, Z., Sillard P., Boucher C., 2002. ITRF2000 A new release of the International
8 Terrestrial Reference Frame for Earth Science Applications. *J. Geophys. Res.*, 107
9 (B10), 2214, 2-19. 10.1029/2001JB00056.
- 10 Anandakrishnan, S., Alley, R.B., Waddington, E.D., 1994. Sensitivity of the ice-divide
11 position in Greenland to climate change, *Geophys. Res. Lett.*, 21(6), 441-444.
- 12 Argus, D., Gordon R., 1991. No-Net Rotational model of current plate velocities
13 incorporating plate motion model NUVEL-1. *Geophys. Res. Lett.*, 18 (11), 2039-
14 2042.
- 15 Brisset, L., and Remy, F., 1996. Antarctica surface topography and kilometric scale
16 features derived from ERS-1 satellite altimeter, *Ann. Glaciol.* 23, 374-381.
- 17 Capra, A., Cefalo, R., Gandolfi, S., Manzoni, G., Tabacco, I.E., Vittuari, L., 2000. Surface
18 topography of Dome Concordia (Antarctica) from kinematic interferential GPS and
19 bedrock topography, *Ann. Glaciol.* 30, 42-46.
- 20 Castellano, E., Becagli, S., Hansson, M., Hutterli, M., Petit, J.R., Rampino, M.R., Severi,
21 M., Steffensen, J.P., Traversi, R., Udisti, R., 2005. Holocene volcanic history
22 recorded in the sulphate stratigraphy of the EPICA-EDC96 ice core (Dome C,
23 Antarctica), *J. Geophys. Res.*, 110 (D06114), DOI:10.129/2004JD005259.
- 24 Cefalo, R., Tabacco, I.E., and Manzoni, G., 1996. Processing of kinematic GPS
25 trajectories at Dome C (Antarctica) and altimetry interpretations, In Unguendoli, M.,
26 ed. *Reports on Surveying and Geodesy*, Bologna, DISTART ed. Nautilus, Università
27 degli Studi di Bologna, 204-222.
- 28 Delmonte, B., Petit, J.R., Andersen, K.K., Basile-Doelsh, I., Maggi, V., Lipenkov, V.Y.,
29 2004. Dust size evidence for opposite regional atmospheric circulation changes over
30 East Antarctica during the Last climatic transition, *Clim. Dynam.* 23, DOI:
31 10.1007/s00382-004-0450-9.

- 1 Dietrich, R., and Rulke, A., 2002. Present status of the SCAR GPS database, In:
2 Proceedings of the SCAR Antarctic Geodesy Symposium AGS'02 on Regional
3 Geodetic Networks, Wellington, New Zealand.
- 4 Eisen, O., Nixdorf, U., Wilhelms, F., Miller, H., 2004. Age estimates of isochronous
5 reflection horizons by combining ice core survey, and synthetic radar data, *J.*
6 *Geophys. Res.* 109 (B4106), DOI:10.1029/2003JB002858.
- 7 EPICA, community members, 2004. Eight Glacial Cycles from an Antarctic Ice Core,
8 *Nature* 429, 623-628.
- 9 Forieri, A., Tabacco, I.E., Della Vedova, A., Zirizzotti, A., Bianchi, C., De Michelis, P., and
10 Passerini, A., 2003. A New Bedrock Map of the Dome C Area, *Terra Antarctica Report*
11 8, 169-170.
- 12 Frezzotti, M., Bitelli, G., de Michelis, P., Deponti, A., Forieri, A., Gandolfi, S., Maggi, V.,
13 Mancini, F., Rémy, F., Tabacco, I.E., Urbini, S., Vittuari, L., Zirizzotti, A, 2004a
14 Geophysical survey at Talos Dôme (East Antarctica): The search for a new deep-
15 drilling site, *Ann. Glaciol.*, 39, 423-432.
- 16 Frezzotti, M., Gandolfi, S., Urbini, S., 2002. Snow megadunes in Antarctica: sedimentary
17 structure and genesis, *J. Geoph. Res.*, 107 (D18), 4344 10.1029/2001JD000673 1-12.
- 18 Frezzotti, M., Pourchet, M., Flora, O., Gandolfi, S., Gay, M., Urbini, S., Vincent, C.,
19 Becagli, S., Gragnani, R., Proposito, M., Severi, M., Traversi, R., Udisti, R., Fily, M.,
20 2004b. New estimations of precipitation and surface sublimation in East Antarctica
21 from snow accumulation measurements, *Clim. Dynam.* 23(7-8), 803-813 DOI:
22 10.1007/s00382-004-0462-5.
- 23 Frezzotti, M., Pourchet, M., Flora, O., Gandolfi, S., Gay, M., Urbini, S., Vincent, C.,
24 Becagli, S., Gragnani, R., Proposito, M., Severi, M., Traversi, R., Udisti, R., Fily, M.,
25 2005. Spatial and temporal variability of snow accumulation in East Antarctica from
26 traverse data, *J. Glaciol.*, 51(207), 113-124.
- 27 Frezzotti, M., Urbini, S., Proposito, M., Scarchilli, C., Gandolfi S., 2007. Spatial and
28 temporal variability of surface mass balance near Talos Dome, East Antarctica. *J.*
29 *Geoph. Res.*, 112 (F02032), DOI:10.1029/2006JF000638.
- 30 Hindmarsh, R.C.A., 1996. Stochastic perturbation of divide position, *Ann. Glaciol.* 23, 94-
31 104.

- 1 Legrand, M., and Delmas, R.J., 1987. A 220-year continuous record of Volcanic H₂SO₄ in
2 the Antarctic ice sheet, *Nature* 327, 671-676.
- 3 Legresy, B., Rignot, E., Tabacco, I.E., 2000. Constraining ice dynamics at Dome C,
4 Antarctica, using remotely sensed measurements, *Geophys. Res. Lett.* 27(21), 3493-
5 3496.
- 6 Leysinger Vieli, G.J.M-C., Siegert, M.J., Payne, A.J., 2004. Reconstructing ice-sheet
7 accumulation rates at ridge B, East Antarctica, *Ann. Glaciol.* 39, 326-330.
- 8 Lorius, C., Merlivat, L., Jouzel, J., and Pourchet, M., 1979. A 30,000 yr isotope climatic
9 record from Antarctic ice, *Nature* 280, 644-648.
- 10 Magand, O., Frezzotti, M., Pourchet, M., Stenni, B., Genoni L., and Fily, M., 2004.
11 Climate variability along latitudinal and longitudinal transects in East Antarctica, *Ann.*
12 *Glaciol.* 39, 351-358.
- 13 Monaghan, A.J., Bromwich, D.H., Fogt, R.L., Wang, S.H., Mayewski, P.A., Dixon, D.A.,
14 Ekaykin, A., Frezzotti, M., Goodwin, I., Isaksson, E., Kaspari, S.D., Morgan, V.I.,
15 Oerter, H., Van Ommen, T., Van der Veen, C.J., Wen, J., 2006. Insignificant
16 Change in Antarctic Snowfall Since the International Geophysical Year, *Science*,
17 313, 827-831.
- 18 Negusini, M., Mancini, F., Gandolfi, S., Capra, A., 2005. Terra Nova Bay GPS permanent
19 station (Antarctica): data quality and first attempt in the evaluation of regional
20 displacement, *J. Geodyn.* 39, 81–90.
- 21 Nereson, N.A., Raymond, C.F., Waddington, E.D., Jacobel, R.W., 1998. Migration of the
22 Siple Dome ice divide, West Antarctica, *J. Glaciol.* 44 (148), 643-652.
- 23 Reijmer, C.H., van den Broeke, M.R., and Scheele, M.P., 2002. Air parcel trajectories and
24 snowfall related to five deep drilling locations in Antarctica based on the ERA-15
25 Dataset, *J. Climate* 15, 1957-1968.
- 26 Rémy, F., and Tabacco, I.E., 2000. Bedrock features and ice flow near the EPICA ice
27 core site (Dome C, Antarctica), *Geophys. Res. Lett.* 27, 405-408.
- 28 Ritz, C., Rommelaere, V., Dumas, C., 2001. Modelling the evolution of Antarctic ice sheet
29 over the last 420,000 years: Implications for the altitude changes in the Vostok region,
30 *J. Geophys. Res.* 106, 31,943-31,964.

- 1 Richardson, C., Aarholt, E., Hamran, S.-E., Holmlund, P., Isaksson, E., 1997. Spatial
2 snow distribution of snow in western Dronning Maud Land, East Antarctica, mapped
3 by a ground based snow radar, *J. Geophys. Res.* 102 (B9), 20,343-20,353.
- 4 Röthlisberger, R., Hutterli, M.A., Sommer, S., Wolff, E.W., and Mulvaney, R., 2000.
5 Factors controlling nitrate in ice cores: Evidence from the Dome C deep ice core, *J.*
6 *Geophys. Res.* 105 (D16), 20565-20572.
- 7 Siegert, M.J., 2003. Glacial-interglacial variations in central East Antarctica ice
8 accumulation rates, *Quater. Sci. Rev.* 22, 741-750.
- 9 Spikes, V.B., Arcone, S., Hamilton, G., Mayewski, P., Dixon, D., Kaspari, S., 2004.
10 Spatial and temporal variability in West Antarctic snow accumulation rates, *Ann.*
11 *Glaciol.* 39, 238-244.
- 12 Stenni, B., Masson-Delmotte, V., Johnsen, S., Jouzel, J., Longinelli, A., Monnin, E.,
13 Röthlisberger, R., and Selmo, E., 2001. An Oceanic Cold Reversal during the last
14 deglaciation, *Science* 293, 2074-2077.
- 15 Stenni, B., Proposito, M., Gagnani, R., Flora, O., Jouzel, J., Falourd, S., and Frezzotti,
16 M., 2002. Eight centuries of volcanic signal and climate change at Talos Dome (East
17 Antarctica), *J. Geoph. Res.* D9 (107), DOI:10.1029/2000JD000317, 1-14.
- 18 Udisti, R., Becagli, S., Castellano, E., Delmonte, B., Jouzel, J., Petit, J.R., Schwander, J.,
19 Stenni, B., and Wolff, E., 2004. Stratigraphic correlations between the European
20 Project for Ice Coring in Antarctica (EPICA) Dome C and Vostok ice cores showing the
21 relative variations of snow accumulation over the past 45 kyr, *J. Geoph. Res.* 109
22 (D8101), DOI:101029/2003JD004180.
- 23 Udisti, R., Becagli, S., Castellano, E., Mulvaney, R., Schwander, J., Torcini, S., and Wolff,
24 E., 2000. Holocene electrical and chemical measurements from the EPICA-Dome C
25 ice core, *Ann. Glaciol.* 30, 20-26.
- 26 Vaughan, D.G., Corr, H.J.F., Doake, C.S.M., Waddington, E.D., 1999. Distortion of
27 isochronous layers in ice revealed by ground-penetrating radar, *Nature* 398 (6725),
28 323-326.
- 29 Vincent, C., and Pourchet, M., 2000. Geodetic measurements and accumulation rate at
30 Dome Concordia, December 1999 and January 2000, Grenoble, Laboratoire del
31 Glaciologie et Géophysique de l'Environnement. Institut Francais pour la Recherche et

1 la Technologie Polaire and for Ente Per La Nuove Tecnologie l'Energia el Ambiente,
2 (Technical report.), 15 pp.

3 Vittuari, L., Vincent, C., Frezzotti, M., Mancini, F., Gandolfi, S., Bitelli, G., Capra, A., 2004.

4 Space geodesy as a tool for measuring ice surface velocity at the Dome C site and
5 between Terra Nova Bay and Dome C (East Antarctica), Ann. Glaciol. 39, 402-408.

6 Young, N.W., Pourchet, M., Kotlyakov, V.M., Korolev, P.A., and Dyugerov, M.B., 1982.

7 Accumulation distribution in the IAGP area, Antarctica: 90°E-150°E, Ann. Glaciol. 3
8 333-338.

9

Deleted:
.....Page Break.....

1 **Figure Captions**

2

3 Fig.1 Schematic map with 500 m contour intervals; the 10 m contours in the Dome C and Talos Dome area
4 are derived from a Digital Elevation Model provided by Brisset and Rémy (1996).

5

6

7 Fig. 2 Comparison of snow accumulation from snow radar (L1 calibrated using the depth-age function at
8 EPICA) versus snow accumulation derived from firn core analysis (β -tritium and Tambora markers:
9 A17 β : β eta marker and A17t: tritium marker) within a 25 km radius of Dome C.

10

11 Fig. 3 Talos Dome snow accumulation map ($\text{kg m}^{-2} \text{yr}^{-1}$) based on snow radar data (S2: 1835-2001 AD).
12 Contour lines of surface topography have a 5 m interval. Snow radar profiles (dotted line), vector ice velocity
13 (red arrow) and prevalent wind direction (blue arrow) are shown. The cyan line indicates the elevation and
14 snow radar profile of Figure 4.

15

16 Fig. 4 Talos Dome snow radar profile from GPR23 to GRP26 (position is shown in Figure 3). Elevation, S1
17 snow radar elevation profile (numbers indicate the depth of the layer) and the 81 yr average of snow
18 accumulation inferred from GPR are shown. Difference in accumulation inferred from GPR for three different
19 periods are shown with error bars.

20

21

22 Fig. 5 Palaeo-accumulation (S3 less S2: 1635-1835 AD grey scale) and present accumulation (Surface less
23 S2: 1835-2001 AD red contour) maps based on snow radar data. Green, blue and black arrows indicate
24 vector of ice velocity acceleration-deceleration and direction of rotation bearing. Contour lines of surface
25 topography have a 5 m interval. Snow radar profiles (dotted line) and prevalent wind direction (blue arrow)
26 are shown.

27

28 Fig. 6 Dome C snow accumulation map ($\text{kg m}^{-2} \text{yr}^{-1}$) based on snow radar data (L5: 1710-2000 AD) and
29 snow accumulation values (in red) derived from firn core analysis (Tritium/ β marker: 1965-2000 AD). Contour
30 lines of surface topography are placed at 2 m intervals. The dashed line indicates snow radar profiles. The
31 cyan line indicates the elevation and snow radar profile of Figure 7.

1

2 Fig. 7 Dome C snow radar profile from SW to NE along the major axis of Dome C (position is reported in
3 Figure 6). Elevation, L5 snow radar elevation profile (numbers indicate the depth of the layer) and the 290 yr
4 average of snow accumulation profile are inferred from GPR. Differences of accumulation inferred from GPR
5 for three different periods are shown with error bars.

6

7 Fig. 8 Temporal variability (5 data average) of D excess and sodium at EPICA EDC96 (from IGBP
8 PAGES/World Data Center for Paleoclimatology Data Contribution Series #2005-048; Röthlisberger et al.,
9 2000; Stenni et al., 2001; Stenni pers. com. 2005), D excess of old Dome C (Lorius et al., 1979) and EPICA
10 EDC96 snow accumulation (1550-1998 AD) from both nssSO₄ volcanic spikes (Castellano et al, 2005) and
11 stake farms (1996-2005 AD).

12

13 Fig. 9 Dome C snow paleo-accumulation map based on snow radar data (L6 less L5: 1602 – 1739 AD). Red
14 contour lines of accumulation map from present back to 1739 AD (Fig. 7). Contour lines of surface
15 topography are placed at 2 m intervals. The dashed line indicates snow radar profiles.

Figure 1

[Click here to download high resolution image](#)

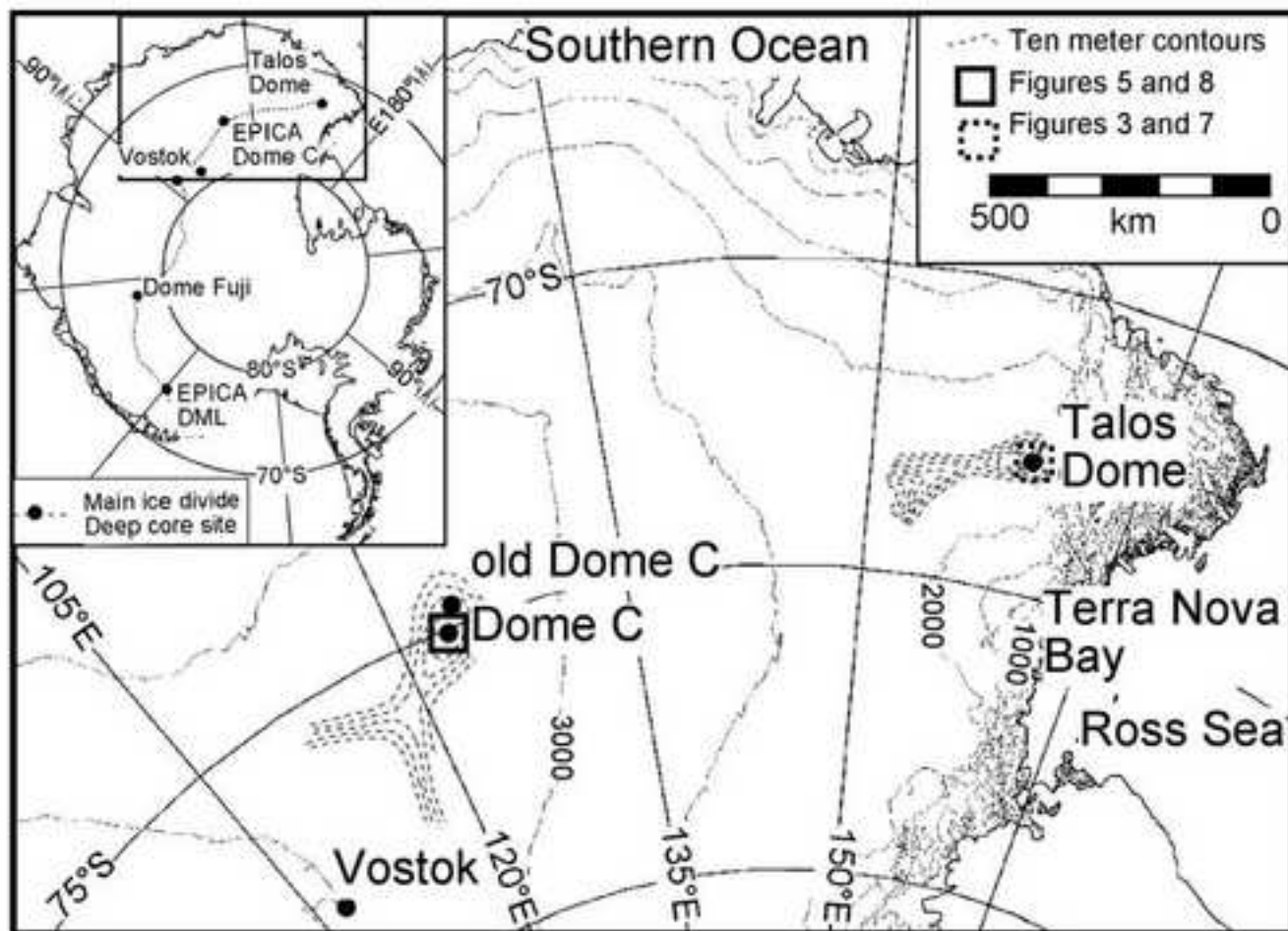


Figure 2

[Click here to download high resolution image](#)

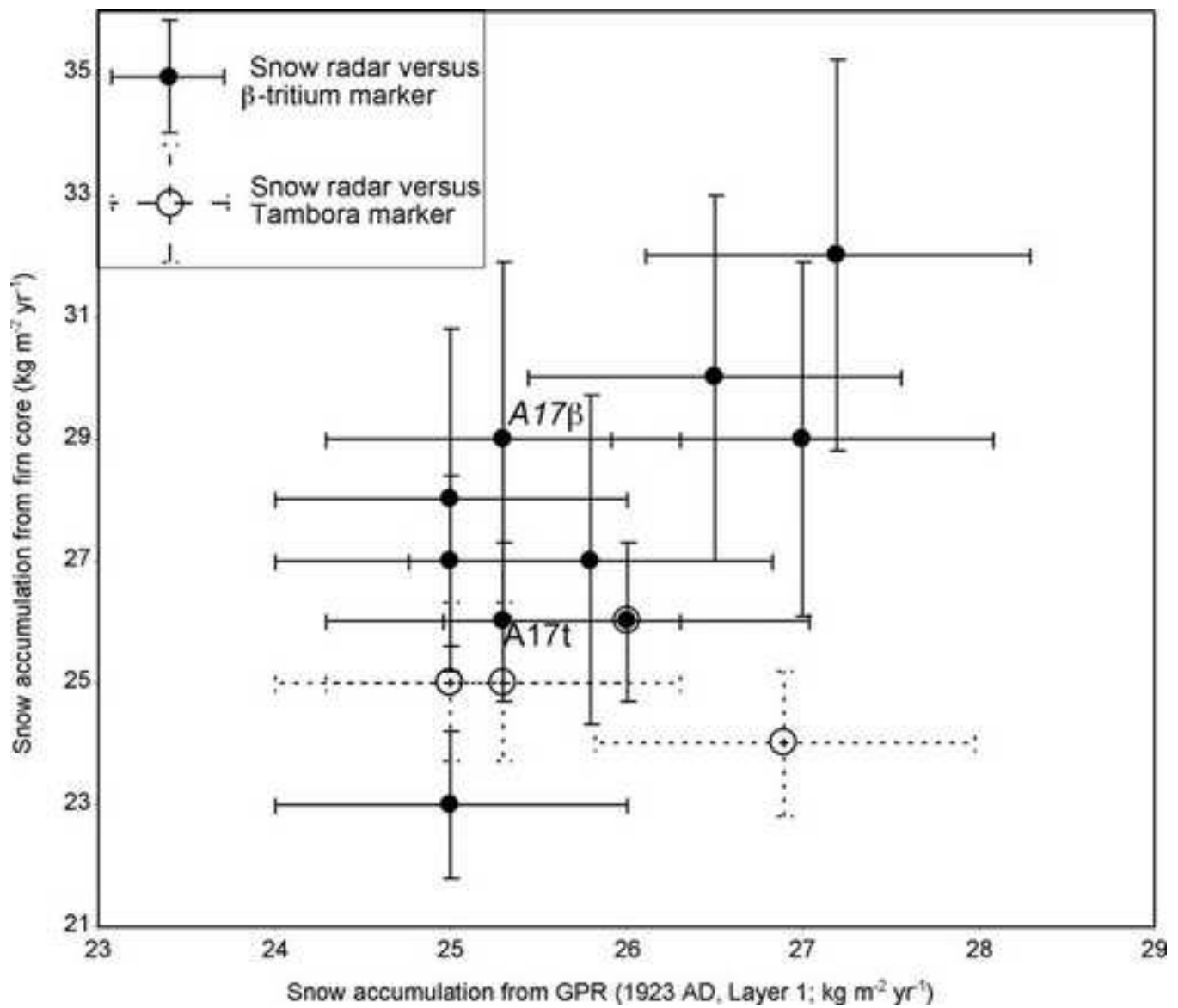


Figure 3
[Click here to download high resolution image](#)

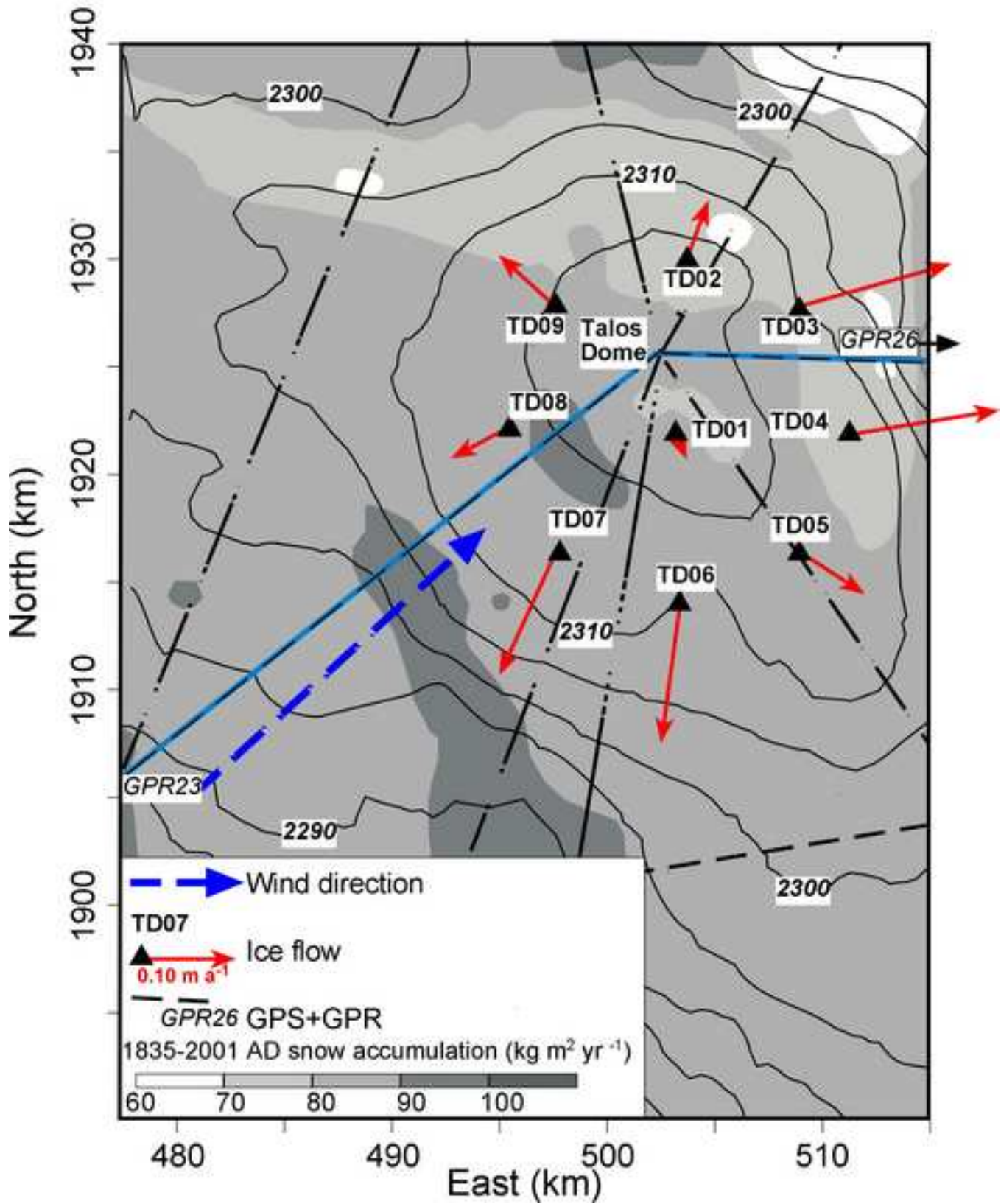


Figure 4

[Click here to download high resolution image](#)

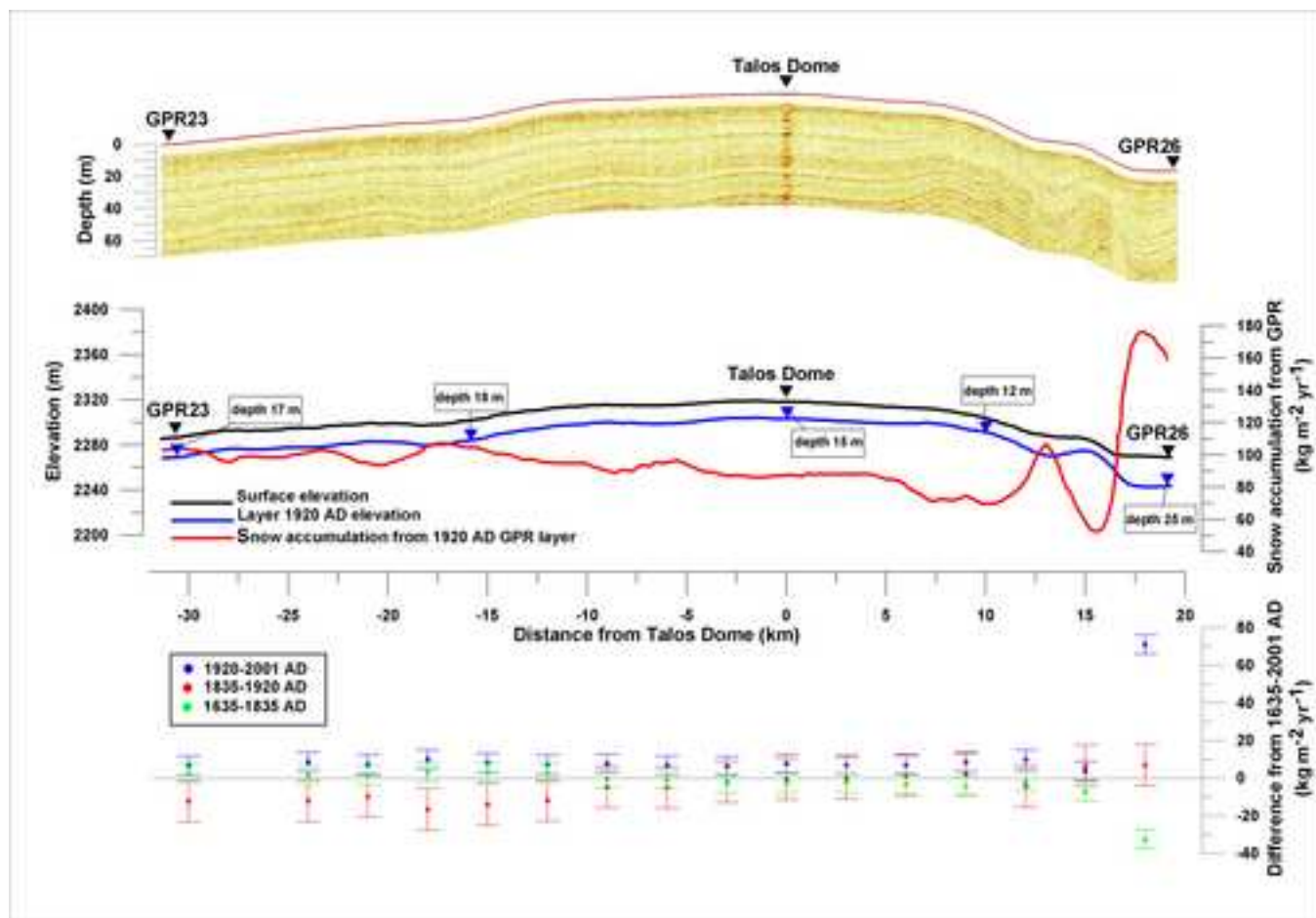


Figure 5
[Click here to download high resolution image](#)

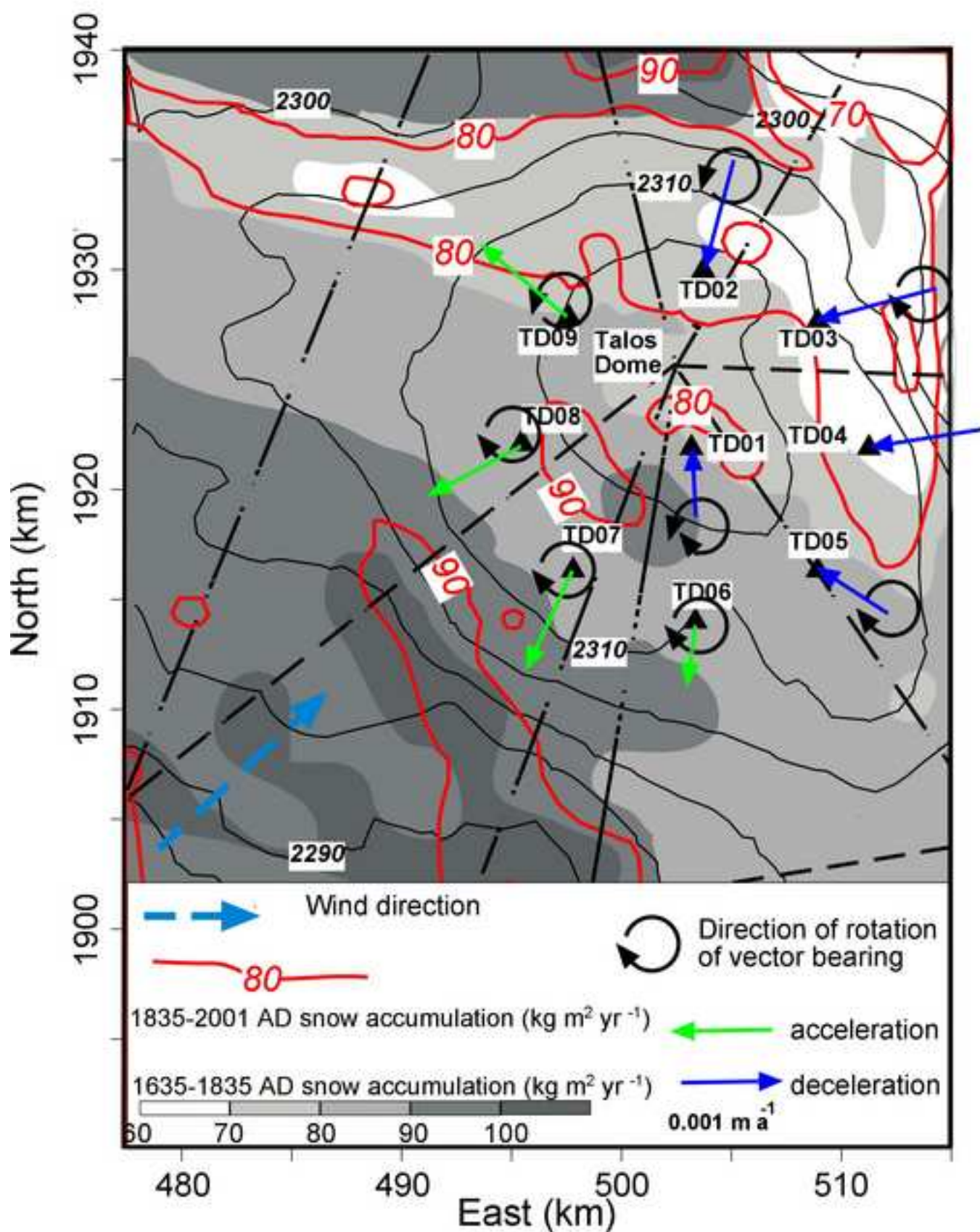


Figure 6
[Click here to download high resolution image](#)

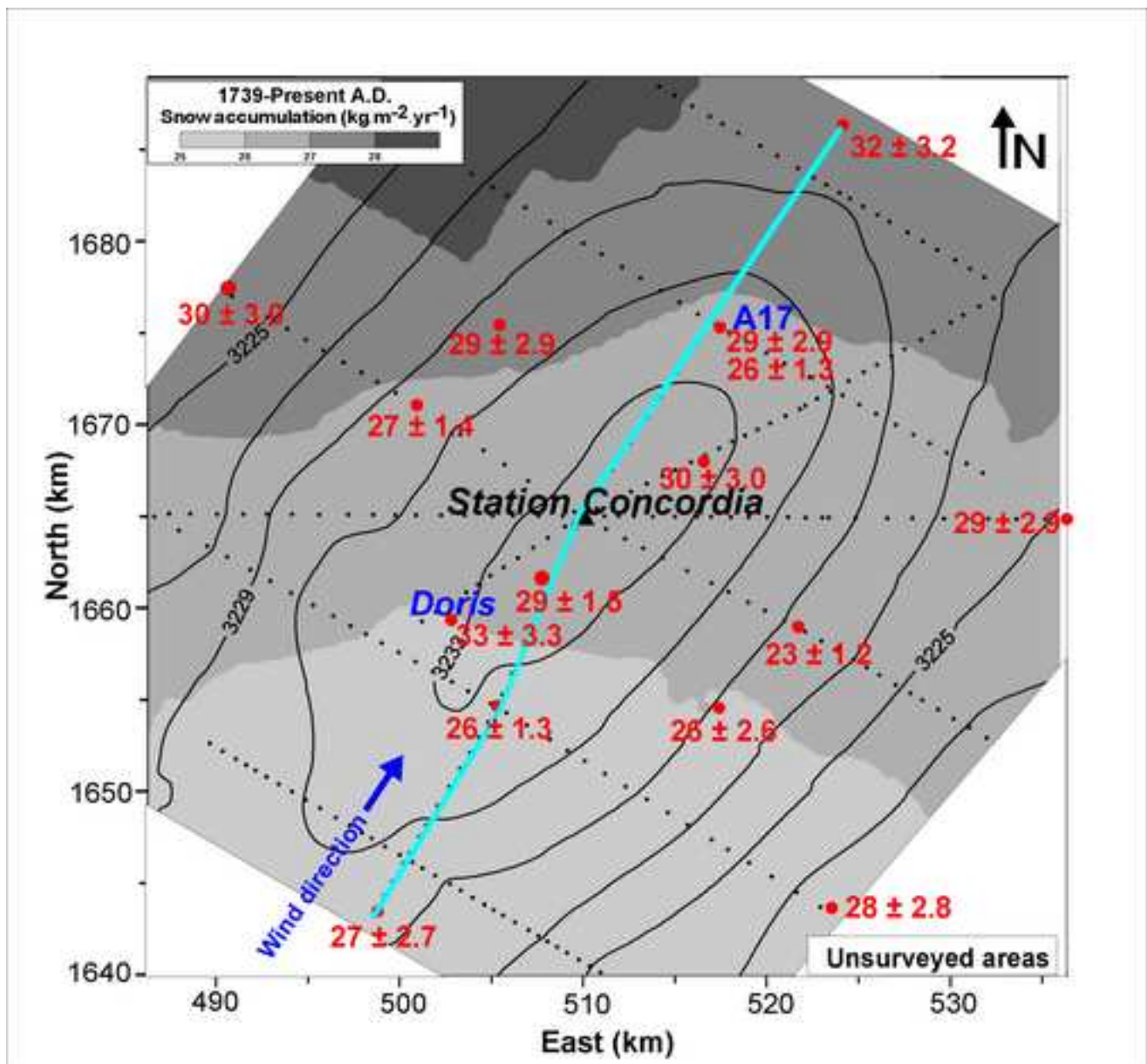


Figure 7

[Click here to download high resolution image](#)

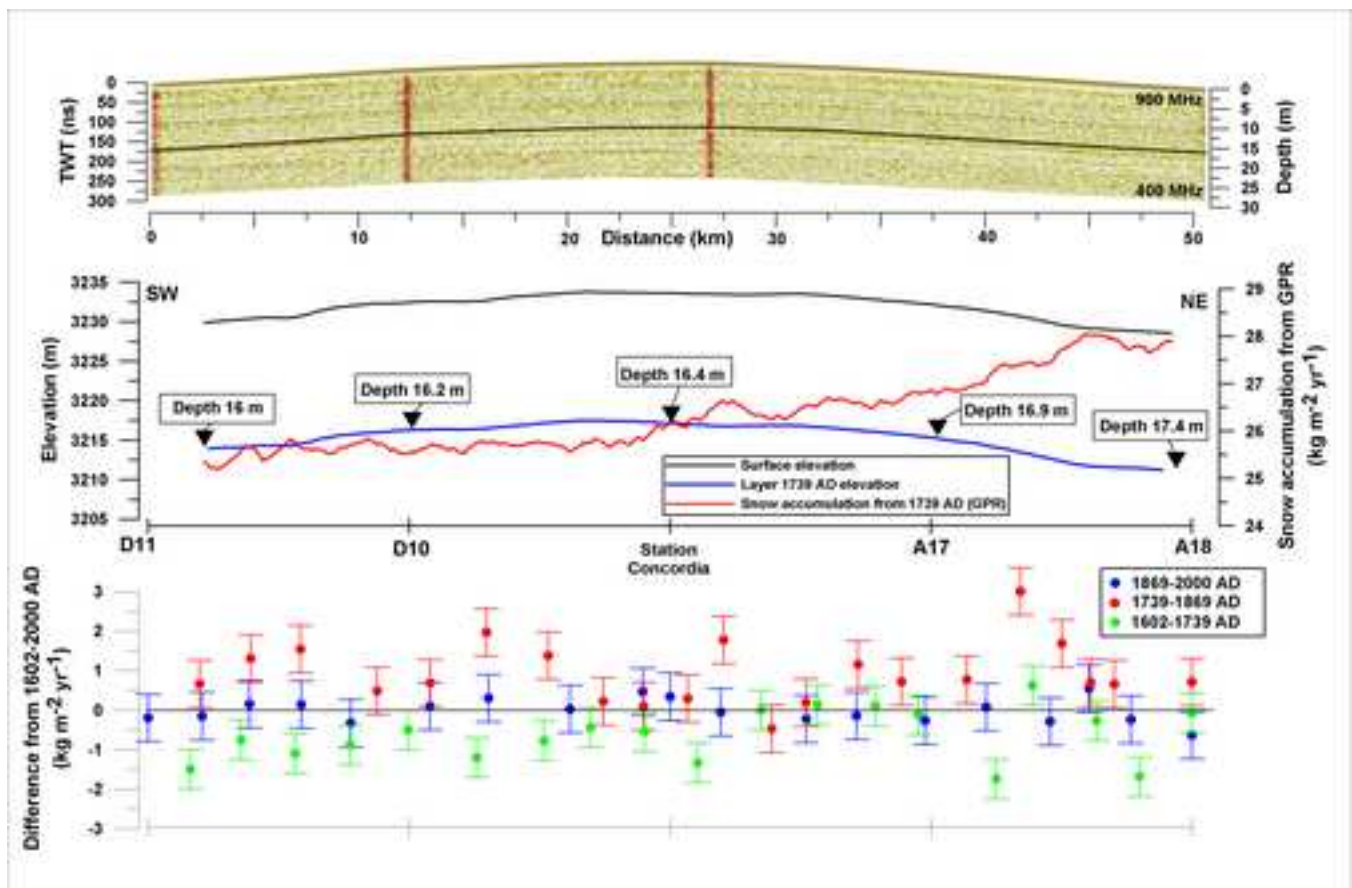


Figure 8
[Click here to download high resolution image](#)

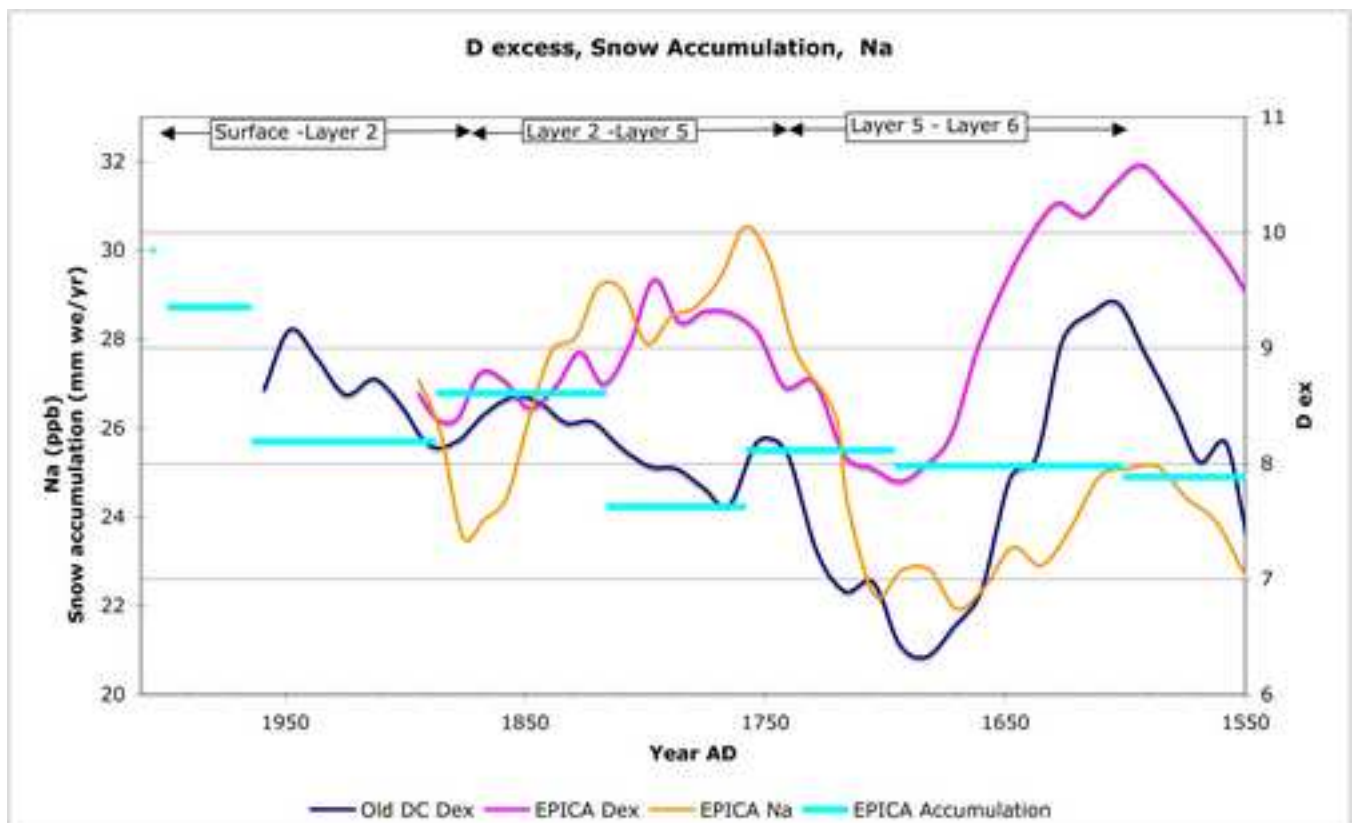
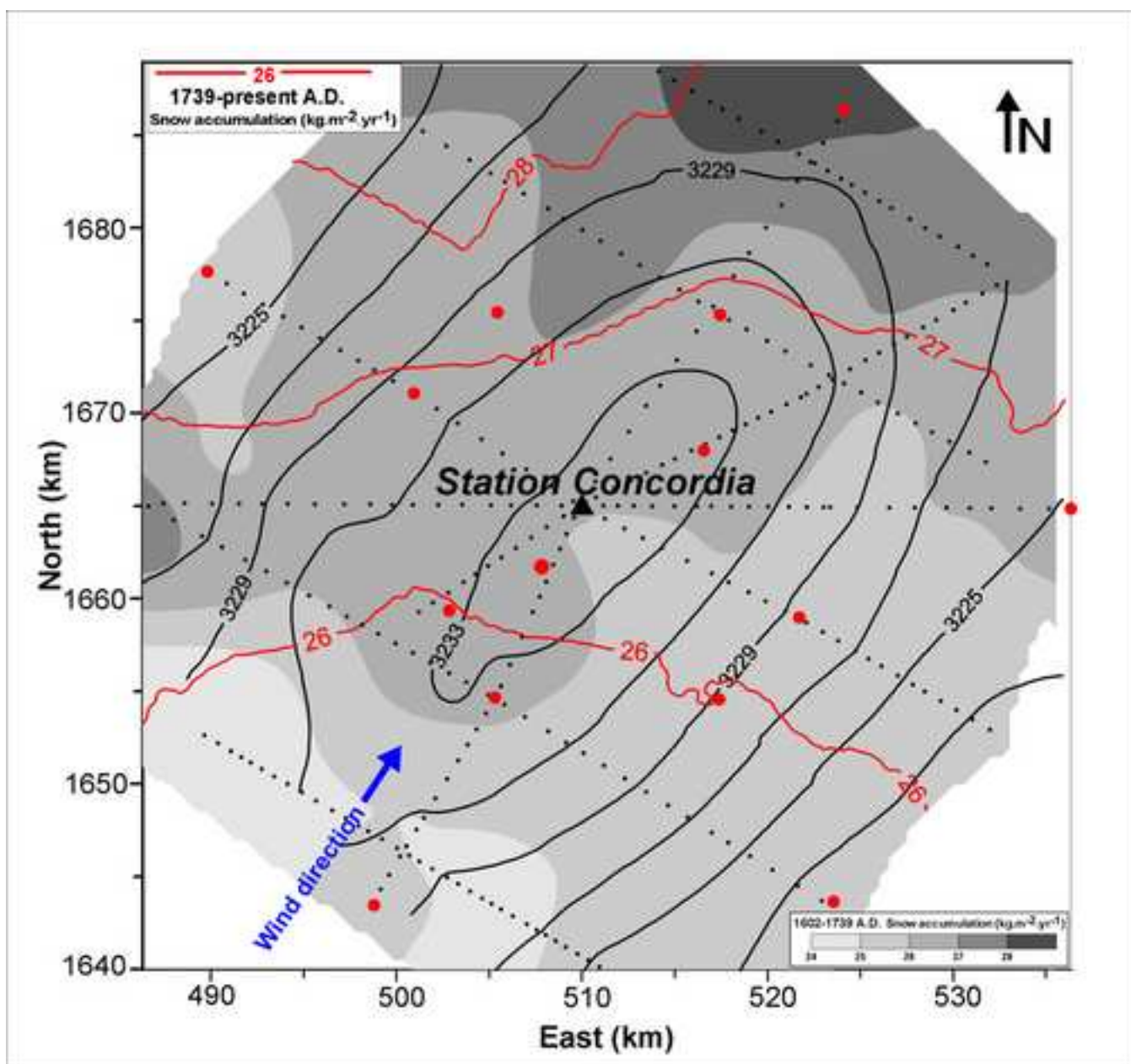


Figure 9
[Click here to download high resolution image](#)



1

2 Table 1 Position (2002 AD) of the stakes at Talos Dome, annual movement (velocity, direction) and
 3 acceleration-deceleration (from 1996-98 to 2002-05 AD).

4

Station ID	Lat S.	Long. E	1996-1998 (δ yr 2.12)	1998-2002 (δ yr 3.03)	2002-2005 (δ yr 3.04)	Acceleration (mm yr ⁻²)
TD01	72°48'03"	159°05'46"				-2±3
Dir. (°)			327	171	177	
Vel. (mm yr ⁻¹)			56±13	40±9	44±9	
TD02	72°43'41"	159°06'45"				-4±3
Dir. (°)			29	15	14	
Vel. (mm yr ⁻¹)			114±13	112±9	90±9	
TD03	72°44'55"	159°16'19"				-5±3
Dir. (°)			76	73	78	
Vel. (mm yr ⁻¹)			343±13	324±9	314±9	
TD04	72°48'04"	159°20'28"				-5±3
Dir. (°)			82	80	82	
Vel. (mm yr ⁻¹)			336±13	302±9	307±9	
TD05	72°51'01"	159°16'21"				-3±3
Dir. (°)			122	125	124	
Vel. (mm yr ⁻¹)			161±13	131±9	143±9	
TD06	72°52'19"	159°05'58"				1±3
Dir. (°)			185	189	191	
Vel. (mm yr ⁻¹)			293±13	301±9	300±9	
TD07	72°51'03"	158°55'38"				3±3
Dir. (°)			202	206	206	
Vel. (mm yr ⁻¹)			270±13	288±9	290±9	
TD08	72°47'59"	158°51'24"				4±3
Dir. (°)			233	246	242	
Vel. (mm yr ⁻¹)			104±13	124±9	125±9	
TD09	72°44'56"	158°55'44"				4±3
Dir. (°)			318	310	305	
Vel. (mm yr ⁻¹)			137±13	156±9	158±9	

5

6